

A Case Study on Improving Capacity Delivery of Battery Packs via Reconfiguration

LIANG HE, EUGENE KIM, and KANG G. SHIN, University of Michigan at Ann Arbor

Cell imbalance in large battery packs degrades their capacity delivery, especially for cells connected in series where the weakest cell dominates their overall capacity. In this article, we present a case study of exploiting system reconfigurations to mitigate the cell imbalance in battery packs. Specifically, instead of using all the cells in a battery pack to support the load, selectively skipping cells to be discharged may actually enhance the pack's capacity delivery. Based on this observation, we propose CSR, a Cell Skipping-assisted Reconfiguration algorithm that identifies the system configuration with (near)-optimal capacity delivery. We evaluate CSR using large-scale emulation based on empirically collected discharge traces of 40 lithium-ion cells. CSR achieves close-to-optimal capacity delivery when the cell imbalance in the battery pack is low and improves the capacity delivery by about 20% and up to 1x in the case of a high imbalance.

CCS Concepts: • **Computer systems organization** → **Embedded software**;

Additional Key Words and Phrases: Reconfigurable battery packs, cell skipping, cell imbalance

ACM Reference Format:

Liang He, Eugene Kim, and Kang G. Shin. 2017. A case study on improving capacity delivery of battery packs via reconfiguration. *ACM Trans. Cyber-Phys. Syst.* 1, 2, Article 11 (February 2017), 23 pages. DOI: <http://dx.doi.org/10.1145/3035539>

1. INTRODUCTION

The ability to provide a high and reliable power supply has made large battery packs widely used in systems such as power grids [Chandra et al. 2014] and electric vehicles (EVs) [Vatanparvar and Faruque 2015]. For example, 7,104 cells are used in Tesla Model S to power the vehicle with 85kWh capacity. However, this large number of cells in the battery pack creates a severe cell imbalance, a notorious but commonly found problem in battery packs. Cell imbalance represents the fact that the strength of cells in accepting/delivering capacity diverges over time and usage, caused by various uncontrollable factors such as manufacturing variability and operational thermal conditions [Barsukov and Qian 2013]. The unbalanced cells degrade their overall capacity delivery, especially for those connected in series (i.e., cell strings)—the cell string is only as strong as its weakest cell [Kim and Shin 2009]. Also, cell imbalance easily leads to their over-charge/discharge, accelerating their capacity fading [Belov and Yang 2008] and causing safety risks such as thermal runaway.

Recently, reconfigurable battery packs, with their ability to dynamically alter the cell connectivity and thus offering a new dimension for system improvement, have

This work was supported in part by NSF under Grants CNS-1329702, CNS-1446117, and LG Chemistry. An early version of this work has been presented at ACM/IEEE e-Energy'16 [He et al. 2016].

Authors' addresses: L. He, E. Kim, and K. G. Shin, Department of Electric Engineering and Computer Science, University of Michigan, 2260 Hayward St., Ann Arbor, MI 48109-2121; emails: {lianghe, kimsun, kgshin}@umich.edu.

Permission to make digital or hard copies of part or all of this work for personal or classroom use is granted without fee provided that copies are not made or distributed for profit or commercial advantage and that copies show this notice on the first page or initial screen of a display along with the full citation. Copyrights for components of this work owned by others than ACM must be honored. Abstracting with credit is permitted. To copy otherwise, to republish, to post on servers, to redistribute to lists, or to use any component of this work in other works requires prior specific permission and/or a fee. Permissions may be requested from Publications Dept., ACM, Inc., 2 Penn Plaza, Suite 701, New York, NY 10121-0701 USA, fax +1 (212) 869-0481, or permissions@acm.org.

© 2017 ACM 2378-962X/2017/02-ART11 \$15.00

DOI: <http://dx.doi.org/10.1145/3035539>

been receiving considerable attention [Badam et al. 2015; He et al. 2014; Kim et al. 2012; Ci et al. 2012a, 2012b]. For example, the physical design of low-complexity reconfigurable battery packs has been explored in Kim et al. [2012], and the tradeoff between cycle efficiency and capacity utilization has been explored in Kim et al. [2011]. System reconfigurability can also be exploited to mitigate the cell imbalance. In this article, we present such a case study of leveraging the JPL-type reconfigurable battery packs [Alahmad et al. 2008] to mitigate the cell imbalance and thus enhance the battery pack’s capacity delivery. We abstract this problem to optimally selecting cells in the pack with the observation that selectively skipping cells to be discharged—thus resting certain cells—may actually improve the battery pack’s capacity delivery over the common approach of using all cells to power the load. Based on this problem abstraction, we propose a cell skipping-assisted reconfiguration (CSR) algorithm that identifies a (near)-optimal system configuration based on cells’ real-time deliverable capacity via dynamic programming (DP), and then further improves it with a genetic algorithm (GA) implementation, if necessary. We also show that CSR reduces the cell imbalance in the long run and is not confined to Jet Propulsion Laboratory (JPL)-type battery packs.

This article makes the following contributions.

- We present the first case study of exploiting system reconfiguration to mitigate cell imbalance in battery packs.
- With two empirically observed sequential properties of cells in the battery pack—one is imposed by the physical direction of discharge current and the other is to avoid the physical short of cells—we abstract the problem of identifying the system configuration with the maximum capacity delivery to a cell-selection problem in the battery pack.
- We design CSR, a two-step reconfiguration algorithm which (i) first assumes ideal cells in the battery pack and identifies the system configuration with near-optimal capacity delivery using DP; (ii) then relaxes the ideal cell assumption and uses a GA implementation to further improve the thus-identified configuration.
- We evaluate CSR with emulation based on the discharge traces of 40 lithium-ion cells, demonstrating about 20% improvement in capacity delivery (up to >100% when facing high cell imbalance).

A preliminary version of this work has been presented in He et al. [2016], and the new materials reported here include: new results on cell imbalance and rate-capacity effect (Section 2.1), new insights on CSR’s near-optimality (Section 5.1.3), a new GA-based design and thus an improved CSR (Section 5.2), new/updated trace-driven emulations (Section 6), and a few further discussions (Section 7).

2. BACKGROUND AND SYSTEM MODEL

In the following text, we introduce the necessary background on battery configuration and the system model.

2.1. Cell Basics

2.1.1. C-Rate of Cells. The discharge current of cells is often expressed as the C-rate. Specifically, the C-rate is a measure of the rate at which the cell is discharged relative to its rated capacity—a 1C rate means the discharge current will drain the cell completely in 1 hour. For example, the 1C rate for a cell with 2,900mAh rated capacity equates to a discharge current of 2,900mA, and a 2C rate would be 5,800mA.

2.1.2. Cell Connectivity and Cell Imbalance. Cells are the basic units of a battery pack. The connectivity among cells determines the battery pack’s output voltage and its capacity delivery. In general, cells in a battery pack can be connected in series or in parallel. The series connection of cells (i.e., a cell string) supplies a voltage that is the

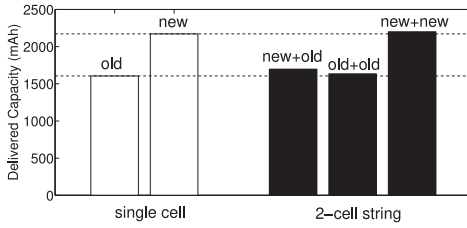


Fig. 1. Capacity delivery of cell string is dominated by the weakest cell.

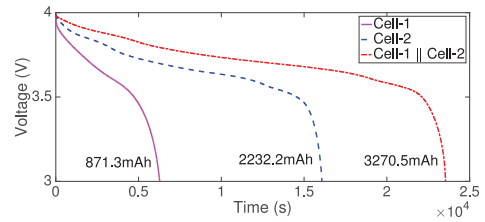


Fig. 2. Parallel connection (denoted by the operator \parallel) delivers the sum of string capacities.

sum of individual cells. Cells connected in series have the same discharge current, and thus the weakest cell dominates their overall capacity delivery—a fundamental physical property inspiring this work. To show this, we collect a set of measurements with four 2,300mAh cells, two of which have been in use over one year (and thus are weaker), and the other two are new (and thus are stronger). Figure 1 plots the delivered capacity when discharging these cells with 1C rate. The new cells deliver 2,171.3mAh capacity on average, while the old cells deliver only 1,605.6mAh. Then, we form three 2-cell strings (i.e., *new-and-old*, *old-and-old*, and *new-and-new*) and again discharge them with 1C rate. A clear observation is that the *new-and-old* string delivers similar capacity as the old cells, validating the string capacity is dominated by the weakest cell. This means not all the capacity of series connected cells can be effectively delivered, and more diverse cell strength leads to more insufficient capacity delivery.

On the other hand, connecting multiple cell strings in parallel does not increase the supplied voltage but splits the discharge current among the strings. The deliverable capacity of parallel strings is the sum of their respective capacities. As a validation, we connect two fully charged cells in parallel—that is, form two parallel 1-cell strings, and discharge them with 500mA current until a cut-off voltage of 3.0V is reached. Figure 2 plots the voltage trace during discharging, together with those when discharging the two cells individually with the same current for comparison. The parallel connection delivers 3,270.5mAh capacity, which is roughly the sum of the two cells' individual capacity but a little larger (i.e., $3,270.5 - (2,232.2 + 871.3) = 167.0$ mAh). This slightly increased capacity delivery can be explained with the rate-capacity effect because the discharge current of individual cells is reduced when connecting them in parallel, as we elaborate later.

Moreover, the diverse cell strength, known as the cell imbalance issue, widely exists in battery packs. We disassembled a 6-cell battery pack used in a laptop and discharged them individually with a constant current. Figure 3(a) shows the capacity delivery of these cells varies from 1,233mAh to 1,482mAh, a difference as large as 20%. Even worse, conventional wisdom says the cell imbalance increases as cells age—their capacity delivery could vary as much as 10x for 5-year cells [Goldberg 2011], as shown in Figure 3(b). To examine this pronounced cell imbalance over time, we discharge another set of lithium-ion cells (same model and purchased in the same batch), which has been in experimental usage for over 3 years, and record their delivered capacity. Figure 3(c) summarizes the experiment results—the strongest cell (i.e., cell-4) delivers 2.54x capacity of the weakest one (i.e., cell-2).

2.1.3. Rate-Capacity Effect and Peukert's Law. The rate-capacity effect—cells' capacity delivery decreases with larger discharge rates—is a unique property of batteries. Figure 4 plots our measurements when discharging four fully charged lithium-ion cells with currents of 0.5C, 1C, and 2C, respectively—smaller discharge currents lead to larger capacity delivery. Cells' rate-capacity effect pronounces with their ages.

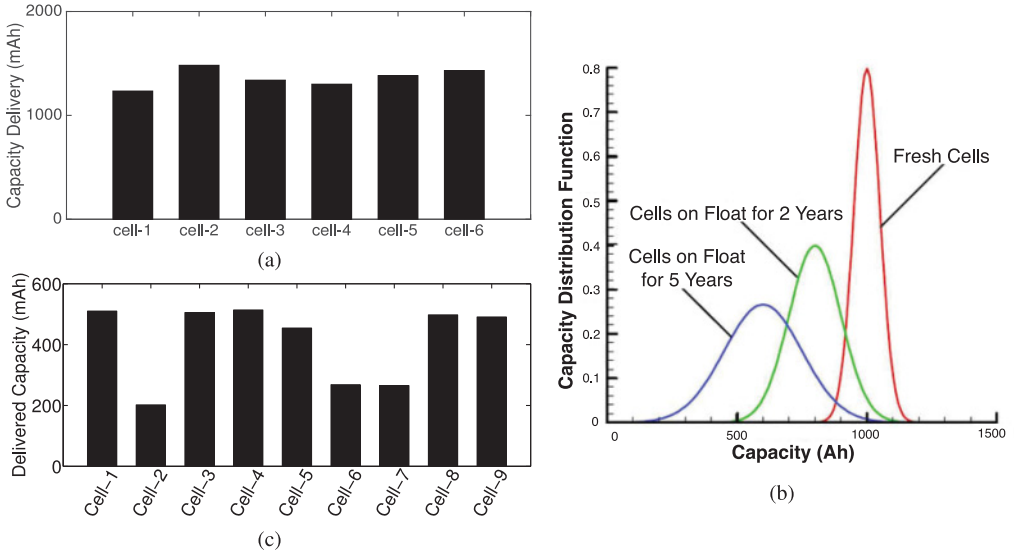


Fig. 3. Cell imbalance: (a) capacity delivery of six cells in a laptop battery pack; (b) cell imbalance increases as aging [Goldberg 2011]; (c) capacity delivery of nine cells in use for over 3 years.

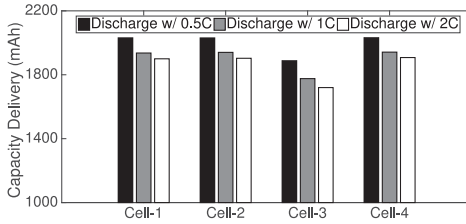


Fig. 4. High discharge rates decrease cell's capacity delivery.

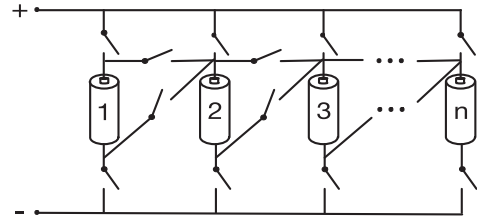


Fig. 5. JPL-type reconfigurable battery packs [Alahmad et al. 2008].

The rate-capacity effect can be mathematically captured by Peukert's Law [Omar et al. 2013] with the basic form of

$$C = I^\alpha t, \quad (1)$$

where C is the cell's rated capacity, I is the discharge rate, t is the actual discharge time, and α ($\alpha \geq 1$) is the Peukert coefficient capturing the cell's nonlinear property—an α of 1 reflects the ideal cells whose capacity delivery is independent to discharge rate (and thus the rate-capacity effect is negligible) and a larger α indicates a pronounced rate-capacity effect. Given rated capacity C and the corresponding discharge rate I , Peukert's law can be extended to estimate a cell's capacity delivery when discharged with I' as

$$C' = C(I/I')^{\alpha-1}. \quad (2)$$

This also allows the estimation of the cells' Peukert coefficient. For example, Figure 4 indicates the Peukert coefficient of Cell-3 is 1.067 at the time of measurement.

2.2. JPL-Type Reconfigurable Battery Packs

In contrast to traditional battery packs with fixed cell connectivity, reconfigurable battery packs offer a new dimension for system optimization with the ability to alter the

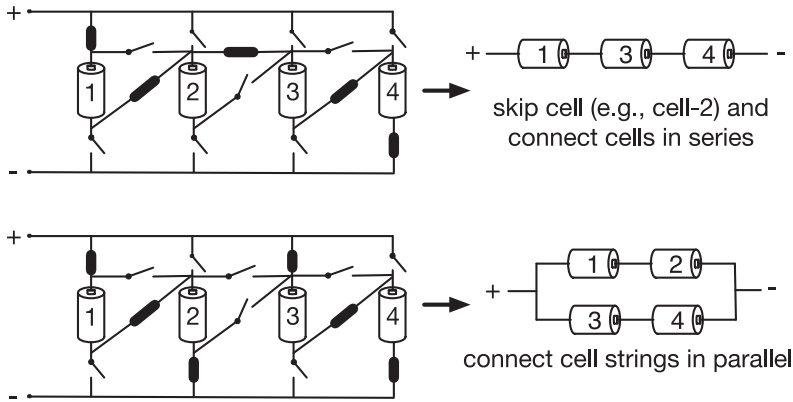


Fig. 6. Adjusting cell connectivity by controlling the open/close states of switches.

connectivity among cells. In this work, we present a case study of exploiting reconfiguration to improve the battery pack's capacity delivery. Specifically, we focus on the reconfigurable battery pack shown in Figure 5 [Alahmad et al. 2008], a classic design by JPL whose similar variations also appeared in Ci et al. [2012b] and Kim and Shin [2010]. By controlling the close/open states of these switches, we can skip cells from discharge, connect cells in series, and connect multiple cell strings in parallel, as illustrated in Figure 6. We refer reconfigurable battery packs designed according to Figure 5 as JPL-type battery packs for presentation convenience.

2.3. System Model

We consider the system model in Figure 7, mainly consisting of the following components.

- Battery pack and load.** A JPL-type battery pack consisting of n cells is used to support load $\langle V, P \rangle$, where V and P are the load required voltage and power, respectively. Each cell in the pack has a nominal voltage v , and thus cell strings consisting of $m = \lceil \frac{V}{v} \rceil$ cells need to be formed to support the load.
- Diodes and regulators.** Each cell string is connected with a diode to regulate the current direction, eliminating the potential safety issues (e.g., reverse charging) caused by the voltage imbalance among multiple strings. Moreover, DC/DC converters are added between the battery pack and the load to ensure a stable voltage supply.¹
- Battery management system (BMS).** During individual charge/discharge cycles as shown in Figure 8, the BMS monitors the real-time cell states, estimates their respective deliverable capacities, and identifies the proper system configuration to support the load. The thus-identified configuration is applied after charging the battery pack, which is then connected to the load and discharged (i.e., the battery pack is reconfigured offline).

Our goal is to design a reconfiguration algorithm for the BMS to identify the system configuration with the maximum capacity delivery, thus prolonging the load operation (e.g., extending the driving range of EVs).

¹Supplying V with cell strings of different sizes via DC/DC conversion is possible but is of lower efficiency due to the larger difference between the supplied and required voltages [Visairo and Kumar 2008].

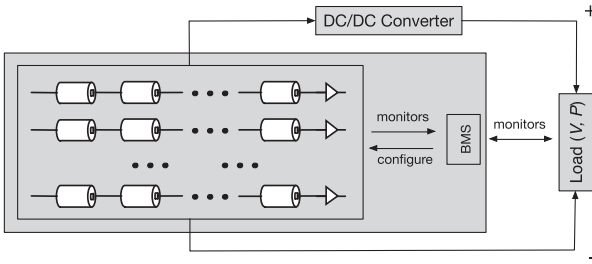


Fig. 7. System model.

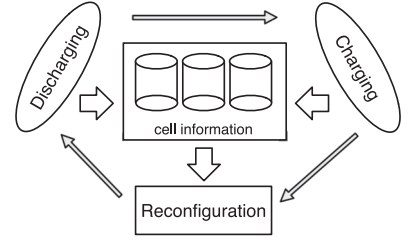


Fig. 8. Application scenario.

Note that altering the system configuration during discharge (i.e., online reconfiguration) is possible in theory, but in practice, the BMS should only reconfigure the system when the load is disconnected and proper safety protections are provided, leading to limited reconfiguration opportunities. This is because the online reconfiguration causes safety risks such as arc flash due to voltage transients or loose connections, and the resultant inrush current could be 50x of the normal current, jeopardizing system safety. Actually, a rule-of-thumb when reconfiguring electricity systems is to de-energize [WPSAC 2007]. The online reconfiguration also incurs non-negligible energy overhead especially for high-load systems such as EVs. As a result, we only consider the scenario of offline reconfiguration in this article, where the safety protections can be provided and reliable external power supply exists. A real-life example for this scenario is to reconfigure the battery pack after charging an EV during night time at home, and then drive it to work the next day.

In the following, we summarize the notations used in this article for the ease of reference.

- n : the number of cells in the battery pack;
- v : the nominal voltage of cells;
- α : Peukert's coefficient capturing the strength of the rate-capacity effect;
- $\langle V, P \rangle$: the load required voltage and power, indicating a required current of $\frac{P}{V}$ and a required cell string size of $m = \lceil \frac{V}{v} \rceil$;
- c_i ($i = 1, 2, \dots, n$): the deliverable capacity of the i th cell under 1C discharge rate;
- C_i ($i = 1, 2, \dots, k$): the deliverable capacity of the i th cell string under 1C discharge rate;
- C_{ideal} : the deliverable capacity of the battery pack with idealized cells, that is, when $\alpha = 1$;
- C_{rc} : the actual deliverable capacity of the battery pack when considering the rate-capacity effect, that is, when $\alpha > 1$.

3. PROBLEM ABSTRACTION

In general, the problem of identifying the system configuration with maximum capacity consisting of two parts is: (i) which cells should be used to support the load; (ii) how these cells should be connected. However, with the physical design of JPL-type battery packs, only the first question needs to be addressed and the answer to the second one follows straightforwardly, because of the sequential properties of cells therein.

Ascendingly indexing cells according to their physical distances to the output terminals as in Figure 5, we observe the following two sequential properties shared by all legal system configurations of JPL-type battery packs. By legal system configuration, we mean (i) it is feasible for the battery pack to achieve such configuration, and (ii) the battery pack can safely support the load with that configuration.

- Intra-String Sequential Property*: for any legal cell string, the indexes of its cells are monotonically increasing. This is because the discharge current is directional and can only pass through cells with smaller indexes before those with larger indexes. Take the 4-cell battery pack in Figure 6 as an example. The cell string $\{1 \rightarrow 3 \rightarrow 2\}$ is not legal, as the current cannot flow reversely from cell-3 to cell-2, indicating this string is not physically achievable.
- Inter-String Sequential Property*: for any legal configuration with parallel cell strings, the indexes of cells in these strings are also monotonic increasing—it is always feasible to index these strings as the 1st string, the 2nd string, and so on, such that for any $i < j$, the indexes of cells in the i th string are smaller than those in the j th string. This inter-string sequential property is to avoid shorting cells in the pack. Again, for the battery pack in Figure 6, the configuration of $\{1 \rightarrow 3\} \parallel \{2 \rightarrow 4\}$ is not legal, as cells in these two strings do not demonstrate a monotonic increasing relationship—using these two strings simultaneously will short cell-2, albeit both of them are physically achievable.

These sequential properties, in turn, lead to the following two observations:

- (1) if a cell is skipped when forming the current string, it cannot be used to form other strings later, and thus its capacity cannot be used to support the load;
- (2) the strings can only be formed sequentially with selected cells according to the increasing order of their indexes—the first m selected cells form the first string, the second m selected cells form the second string, and so on, where $m = \lceil \frac{V}{v} \rceil$ is the number of series cells required by the load.

These further lead to the following problem abstraction: for JPL-type battery packs, the problem of identifying the configuration with maximum capacity delivery is equivalent to optimally determining which cells should be used to support the load, after which the question of how to connect these selected cells can be answered accordingly. Figure 9 shows an example on the problem abstraction with a JPL-type battery pack consisting of the nine cells in Figure 3(c) and the load requires 3-cell strings—if we decide to skip cell-2, cell-6, and cell-7 from discharge, the system configuration is also determined by sequentially forming the strings with the remaining cells, that is, $\{1 \rightarrow 3 \rightarrow 4\} \parallel \{5 \rightarrow 8 \rightarrow 9\}$.

4. WHY TO SKIP CELLS?

Intuitively, we want to use all the cells in the battery pack (thus forming the maximum number of cell strings) to support the load, especially in view of the rate-capacity effect—more parallel strings reduce the discharge rate of individual cells and thus improve their capacity delivery.

However, the widely existing cell imbalance, together with the fact that the weakest cell dominates the string's capacity delivery, lead to the observation that sometimes selectively skipping cells to be discharged may improve the battery pack's capacity delivery. Let us again consider the JPL-type battery pack in Figure 9, in which the deliverable capacities of cells under 1C discharge rate are listed. When all these nine cells are used, we can form three 3-cell strings to support the load in parallel: $\{1 \rightarrow 2 \rightarrow 3\} \parallel \{4 \rightarrow 5 \rightarrow 6\} \parallel \{7 \rightarrow 8 \rightarrow 9\}$ (Figure 10). The deliverable capacity of these strings are 202mAh (dominated by cell-2), 268mAh (dominated by cell-6), and 265mAh (dominated by cell-7), respectively. However, if we skip cell-2, cell-6, and cell-7 from discharge, we can form two cell strings $\{1 \rightarrow 3 \rightarrow 4\}$ and $\{5 \rightarrow 8 \rightarrow 9\}$ with a total deliverable capacity of $505 + 491 = 996$ mAh, which is 35% more when compared with using all the cells (i.e., $202 + 268 + 265 = 735$ mAh).

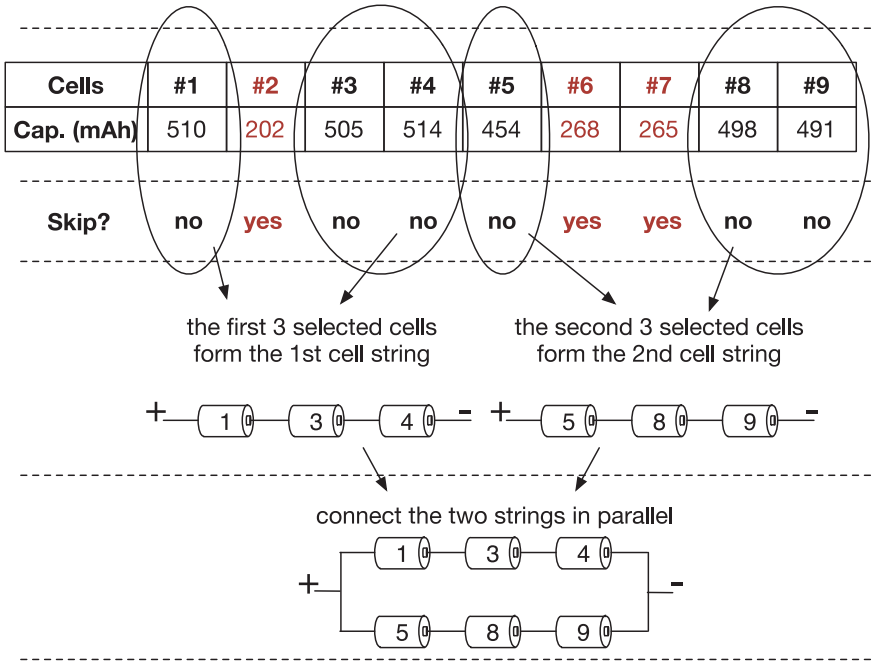


Fig. 9. Illustrative example on abstracting the problem of identifying the optimal configuration to determine which cells to skip.

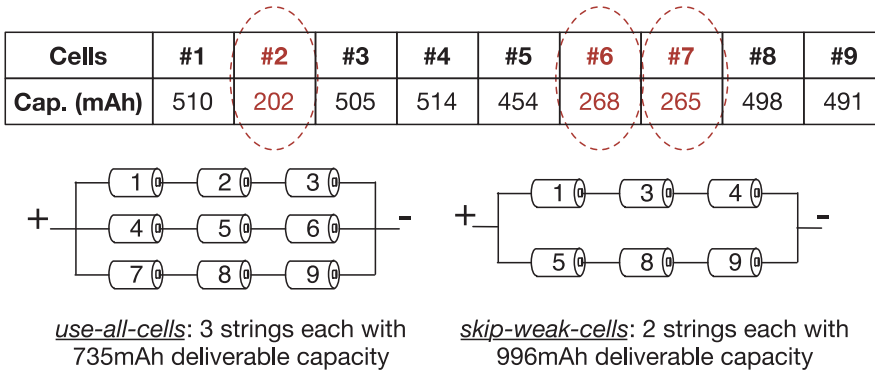


Fig. 10. Illustrative example: skipping cells from discharge may improve the battery pack’s capacity delivery.

The problem becomes trickier when considering the rate-capacity effect. Two strings are formed in the aforementioned example when cells are skipped, meaning each remaining cell needs to supply a current of $\frac{P}{2V}$ to the load. On the other hand, three strings are formed when all cells are used, and thus each cell only needs to supply a current of $\frac{P}{3V}$. By Peukert’s law (Equation (2)), we know the actual capacity delivery of the battery pack is $996 \times (2V \cdot I_C/P)^{\alpha-1}$ when skipping cells and $735 \times (3V \cdot I_C/P)^{\alpha-1}$ when using all the cells, where I_C is the 1C discharge rate in Amps—there is no one-for-all answer to which one is larger without the knowledge on V , P , and α .

The aforementioned example reveals a dilemma when selecting cells to support the load: selectively skipping cells may increase the capacity delivery with ideal cells but

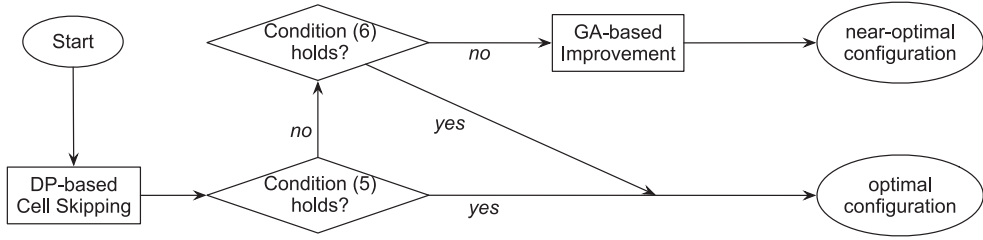


Fig. 11. Flow chart of CSR.

forms fewer parallel strings, which, on the other hand, increases cells' discharge rate and thus degrades their capacity delivery due to the rate-capacity effect.²

5. CELL SKIPPING-ASSISTED RECONFIGURATION

Denote cells' deliverable capacity under 1C rate as $\langle c_1, c_2, \dots, c_n \rangle (c_i > 0)$, which can be measured from their previous discharge cycle.³ CSR identifies the battery pack configuration with two steps: it first uses a DP-based method to determine which, if any, cells should be skipped from discharge, identifying the configuration with the maximum capacity delivery under certain conditions (e.g., when the rate-capacity effect is negligible); CSR then uses a GA implementation to further improve the thus-identified configuration if needed. Figure 11 shows the flow chart of CSR.

5.1. Step I: DP-Based Cell Skipping

For the ease of description, let us first assume ideal cells (i.e., $\alpha = 1$ and the rate-capacity effect is negligible) in the battery pack.

5.1.1. The DP Design. Define a cell skipping vector $S_{1 \times n} = \{s_i\} (i = 1, 2, \dots, n)$ as

$$s_i = \begin{cases} 1 & \text{if the } i\text{th cell is skipped from discharge,} \\ 0 & \text{otherwise.} \end{cases}$$

From Section 3, we know any instance of $S_{1 \times n}$ also defines a system configuration.

Moreover, the sequential properties of cells allow us to identify the optimal configuration of an n -cell battery pack $S_{1 \times n}^*$ based on the optimal configurations when considering only its first $(n - i)$ ($i = 1, 2, \dots, m - 1$) cells $S_{1 \times (n-i)}^*$ —the optimal substructure of DP.

Define $H_m(i, j)$ ($j - i \geq m - 2$) as the largest $(m - 1)$ elements among $\{c_i, c_{i+1}, \dots, c_j\}$. Further define $g_m(i, j)$ as the deliverable capacity of the string formed by the j th cell and the cells corresponding to $H_m(i, j)$. Specifically,

$$g_m(i, j) = \min\{H_m(i, j - 1), c_j\} (i = 1, 2, \dots, n - m + 1; j = m + i - 1, m + i, \dots, n). \quad (3)$$

Define $f_m(j)$ ($j = 1, 2, \dots, n$) as the maximum deliverable capacity when only considering the first j cells in the pack to support the load, and cell- j is not skipped (i.e., $s_j = 0$), meaning cell- j is the last cell of an m -cell string. Clearly,

$$f_m(1) = f_m(2) = \dots = f_m(m - 1) = 0.$$

²Note that the three weakest cells in the pack are skipped from discharge to facilitate the illustration in the example shown in Figure 10. In practice, however, greedily skipping the weakest cells is not always the best solution, as we will see in Section 6.

³CSR does not strictly require cells' capacity delivery under 1C rate as the input—the capacity delivery of cells under any unified discharge rate, for example, the load required current $\frac{P}{V}$, serves the purpose.

$g_{m=3}(i, j)$	$j=1$	$j=2$	$j=3$	$j=4$	$j=5$	$j=6$	$j=7$	$j=8$	$j=9$
$i=1$	-	-	202 (1, 2, 3)	505 (1, 3, 4)	454 (1, 4, 5)	268 (1, 4, 6)	265 (1, 4, 7)	498 (1, 4, 8)	491 (1, 4, 9)
$i=2$	-	-	-	202 (2, 3, 4)	454 (3, 4, 5)	268 (3, 4, 6)	265 (3, 4, 7)	498 (3, 4, 8)	491 (3, 4, 9)
$i=3$	-	-	-	-	454 (3, 4, 5)	268 (3, 4, 6)	265 (3, 4, 7)	498 (3, 4, 8)	491 (3, 4, 9)
$i=4$	-	-	-	-	-	268 (4, 5, 6)	265 (4, 5, 7)	454 (4, 5, 8)	491 (4, 8, 9)
$i=5$	-	-	-	-	-	-	265 (5, 6, 7)	268 (5, 6, 8)	454 (5, 8, 9)
$i=6$	-	-	-	-	-	-	-	265 (6, 7, 8)	268 (6, 7, 9)
$i=7$	-	-	-	-	-	-	-	-	265 (7, 8, 9)
$i=8$	-	-	-	-	-	-	-	-	-
$i=9$	-	-	-	-	-	-	-	-	-
$f_{m=3}(j)$	0 (-, -)	0 (-, -)	202 (-, g(1, 3))	505 (-, g(1, 4))	454 (3, g(3, 5))	470 (4, g(4, 6))	770 (4, g(5, 7))	773 (4, g(5, 8))	959 (4, g(5, 9))

Fig. 12. A walk-through example on CSR ($n = 9, m = 3$).

Further defining $f_m(0) = 0$, we have the following optimal substructure based on which the system configuration with maximum deliverable capacity can be identified

$$f_m(j) = \max\{f_m(i) + g_m(i + 1, j)\} \quad (j = m, m + 1, \dots, n; i = 0, 1, \dots, j - m). \quad (4)$$

Clearly, the maximum capacity delivery of ideal battery packs is $\mathbb{C}_{\text{ideal}}^{\text{dp}} = \max\{f_m(j)\}$, and the corresponding configuration $S_{1 \times n}^{\text{dp}}$ can be identified via reversing the search from $j^{\text{dp}} = \max_j\{f_m(j)\}$. The DP-based cell skipping requires a space complexity of $O(n^2)$ and a computation complexity of $O(mn^2 \lg n)$ —both dominated by the space/computation to store/calculate $g_m(i, j)$ s.

5.1.2. Walk-Through Example. Next, we use a walk-through example, based on the 9-cell battery pack in Figure 10, to facilitate the understanding of the DP-based cell skipping. Let us first consider $g_{m=3}(i, j)$. For example, when $i = 2$ and $j = 7$, $g_{m=3}(2, 7)$ returns the capacity of the string formed by the $m - 1 = 2$ cells from cell-2 to cell-(7-1) = 6 with the maximum deliverable capacity (i.e., $H_{m=3}(2, 6)$), and with cell-7 as the last cell. Specifically,

$$g_{m=3}(2, 7) = \min\{H_{m=3}(2, 6), c_7\}.$$

As $H_{m=3}(2, 6)$ is the largest of the two elements among

$$\{c_2, c_3, \dots, c_6\} = \{202, 505, 514, 454, 268\},$$

we know $H_{m=3}(2, 6) = \{505, 514\}$ and

$$g_{m=3}(2, 7) = \min\{505, 514, 265\} = 265.$$

Similarly, we know

$$g_{m=3}(2, 8) = \min\{H_{m=3}(2, 7), c_8\} = \min\{505, 514, 498\} = 498.$$

Other $g_{m=3}(i, j)$ s can be calculated similarly, as summarized in Figure 12. Figure 12 also lists the corresponding selected cells for each $g_{m=3}(i, j)$ s. For example,

$$g_{m=3}(2, 7) = 265 (3, 4, 7)$$

means cell-3, cell-4, and cell-7 are selected to form the string, delivering 265mAh capacity. This way, $f_{m=3}(j)$ s can be iteratively calculated according to Equation (4). For example,

$$f_{m=3}(3) = f_{m=3}(0) + g_{m=3}(1, 3) = 202,$$

$$f_{m=3}(4) = \max \left\{ \begin{array}{l} f_{m=3}(0) + g_{m=3}(1, 4), \\ f_{m=3}(1) + g_{m=3}(2, 4) \end{array} \right\} = \max\{202, 505\} = 505,$$

$$f_{m=3}(5) = \max \left\{ \begin{array}{l} f_{m=3}(0) + g_{m=3}(1, 5), \\ f_{m=3}(1) + g_{m=3}(2, 5), \\ f_{m=3}(2) + g_{m=3}(3, 5) \end{array} \right\} = \max\{454, 454, 454\} = 454.$$

Other $f_{m=3}(j)$ s, together with how they are obtained, are also summarized in Figure 12. For example,

$$f_{m=3}(8) = 773 (4, g(5, 8))$$

means $f_{m=3}(8)$ is obtained based on $f_{m=3}(4)$ and $g_{m=3}(5, 8)$. As $f_{m=3}(9) = 959$ is the maximum of $f_{m=3}(j)$ s, we know the configuration with maximum capacity uses cell-9 as the last cell. This way, we reverse the search from $f_{m=3}(9)$ and find

$$f_{m=3}(9) = f_{m=3}(4) + g_{m=3}(5, 9) = g_{m=3}(1, 4) + g_{m=3}(5, 9).$$

From Figure 12, we know cell-1, cell-3, and cell-4 are used to form the string of $g_{m=3}(1, 4)$, while those for $g_{m=3}(5, 9)$ are cell-5, cell-8, and cell-9, indicating an identified configuration of

$$\{1 \rightarrow 3 \rightarrow 4\} \parallel \{5 \rightarrow 8 \rightarrow 9\},$$

and a skipping vector

$$S_{1 \times 9}^{\text{dp}} = \{0, 1, 0, 0, 0, 1, 1, 0, 0\}.$$

5.1.3. (Near)-Optimality Analysis. The DP-based cell skipping identifies the battery pack configuration with the maximum capacity delivery for ideal cells (i.e., $\alpha = 1$). In the following, we prove its bounded near-optimality in capacity delivery even for cells with $\alpha > 1$.

First, we have the following lemma on the capacity delivery of a given configuration when considering the rate-capacity effect. Note that this is also the capacity delivery for non-reconfigurable battery packs.

LEMMA 5.1. *For any configuration with k ($1 \leq k \leq \lfloor \frac{n}{m} \rfloor$) parallel m -cell strings, denote the deliverable capacity of these k strings (in ascending order) under 1C discharge rate as*

$$C_1 \leq C_2 \leq \dots \leq C_k,$$

and further define $C_{\text{ideal}} = \sum_{i=1}^k C_i$. When using this configuration to support load $\langle V, P \rangle$, its actual deliverable capacity C_{rc} when considering the rate-capacity effect is

$$C_{\text{rc}} = (V \cdot I_C / P)^{\alpha-1} \sum_{i=1}^k (k-i+1)^\alpha (C_i - C_{i-1}).$$

where I_C is the 1C discharge current in amps.

PROOF. The entire discharge process can be divided into k phases when these k strings are connected in parallel to support the load.

—*Phase-1:* The Phase-1 of the discharge process starts when the discharge begins and ends when the weakest cell string (i.e., the one with deliverable capacity C_1) depletes. During this phase, the load is supported with k parallel strings, and each of the strings has a discharge rate of $I_1 = \frac{P}{k \cdot V}$. By Peukert's law,⁴ the delivered capacity during this phase is

$$k \cdot C_1 (I_C / I_1)^{\alpha-1}.$$

⁴Note that both Peukert's law and Peukert's coefficient are only used to analytically track the (near)-optimality, but are not required when implementing.

—*Phase-2*: This discharge phase starts from the depletion of the weakest string and ends when the second weakest string (i.e., the one with deliverable capacity C_2) is drained. Only $(k - 1)$ parallel strings are available to support the load during this phase, leading to a discharge rate of $I_2 = \frac{P}{(k-1)V}$ for each string. This way, the delivered capacity during Phase-2 is

$$(k - 1) \cdot (C_2 - C_1) (I_C / I_2)^{\alpha-1}.$$

—.....

—*Phase-k*: The last discharge phase is when only the strongest cell string (i.e., the one with deliverable capacity C_k) is available to support the load. During this phase, the strongest string has a discharge rate of $I_k = \frac{P}{1V}$ and the delivered capacity is

$$1 \cdot (C_k - C_{k-1}) (I_C / I_k)^{\alpha-1}.$$

Further defining $C_0 = 0$, the deliverable capacity of the configuration when considering the rate-capacity is

$$\mathbb{C}_{rc} = \sum_{i=1}^k (k - i + 1) (C_i - C_{i-1}) (I_C / I_i)^{\alpha-1} = (V \cdot I_C / P)^{\alpha-1} \sum_{i=1}^k (k - i + 1)^\alpha (C_i - C_{i-1}). \quad \square$$

Lemma 5.1, in turn, leads to the following lemma on the maximum deliverable capacity \mathbb{C}_{rc} of any configuration with given \mathbb{C}_{ideal} .

LEMMA 5.2. *For any configuration with given \mathbb{C}_{ideal} ,*

$$\mathbb{C}_{rc} \leq \mathbb{C}_{ideal} (k \cdot V \cdot I_C / P)^{\alpha-1}.$$

Furthermore, when $\alpha > 1$, the equality holds if and only if

$$C_1 = C_2 = \dots = C_k = \mathbb{C}_{ideal} / k.$$

PROOF. It is clear that $\mathbb{C}_{rc} = \mathbb{C}_{ideal} (k \cdot V \cdot I_C / P)^{\alpha-1}$ when $C_1 = C_2 = \dots = C_k = \mathbb{C}_{ideal} / k$. To show $\mathbb{C}_{ideal} (k \cdot V \cdot I_C / P)^{\alpha-1}$ is also the maximum capacity delivery with given \mathbb{C}_{ideal} , we define

$$\delta_i = C_i - C_{i-1} \quad (i = 1, 2, \dots, k),$$

and thus

$$k\delta_1 + (k - 1)\delta_2 + \dots + \delta_k = \mathbb{C}_{ideal}.$$

Denote \mathbb{C}_{rc}^1 as the capacity delivery of the configuration with $C_1 = C_2 = \dots = C_k = \mathbb{C}_{ideal} / k$, and \mathbb{C}_{rc}^2 as the capacity delivery of any other configurations with \mathbb{C}_{ideal} , we have

$$\begin{aligned} \mathbb{C}_{rc}^1 - \mathbb{C}_{rc}^2 &= (V \cdot I_C / P)^{\alpha-1} k^{\alpha-1} \mathbb{C}_{ideal} - (V \cdot I_C / P)^{\alpha-1} \sum_{i=1}^k (k - i + 1)^\alpha (C_i - C_{i-1}) \\ &= (V \cdot I_C / P)^{\alpha-1} [k^{\alpha-1} (k\delta_1 + (k - 1)\delta_2 + \dots + \delta_k) - (k^\alpha \delta_1 + (k - 1)^\alpha \delta_2 + \dots + \delta_k)] \\ &= (V \cdot I_C / P)^{\alpha-1} [(k - 1)(k^{\alpha-1} - (k - 1)^{\alpha-1})\delta_2 + (k - 2)(k^{\alpha-1} - (k - 2)^{\alpha-1})\delta_3 + \dots + (k^{\alpha-1} - 1)\delta_k] \\ &\geq 0, \end{aligned}$$

and thus the theorem follows. \square

Lemma 5.2 indicates that with a given \mathbb{C}_{ideal} , the battery pack's actual capacity delivery is maximized when the parallel cell strings are of similar strength. We have the following theorem on the upper bound of the battery pack's capacity delivery based on Lemma 5.2.

THEOREM 5.3. *Denote \mathbb{C}_{rc}^* as the maximum capacity delivery of the battery pack, then*

$$\mathbb{C}_{rc}^* \leq (V \cdot I_C/P)^{\alpha-1} \lfloor n/m \rfloor^{\alpha-1} \mathbb{C}_{ideal}^{dp},$$

where \mathbb{C}_{ideal}^{dp} is the idealized capacity delivery identified by the DP-based cell skipping.

PROOF. From Lemma 5.2, we know the battery pack's capacity delivery is maximized when (i) its idealized capacity delivery \mathbb{C}_{ideal} is maximized; and (ii) the maximum number of cell strings are formed (i.e., k is maximized) and they deliver the same capacity. As the DP-based cell skipping identifies the configuration with maximum capacity delivery when the cells are ideal, we know

$$\mathbb{C}_{ideal} \leq \mathbb{C}_{ideal}^{dp}.$$

Furthermore, it is clear that

$$k \leq \lfloor n/m \rfloor.$$

The theorem follows by combining these with Lemma 5.2. \square

Next, we consider the lower bound of the actual capacity delivery of the configuration identified by the DP-based method, consisting of k^{dp} parallel strings. Intuitively, its capacity delivery is minimized when we sequentially use the k^{dp} strings to support the load instead of discharging them in parallel, resulting in the largest possible discharge current of individual cells (i.e., $\frac{P}{V}$).

THEOREM 5.4. *For the configuration identified by the DP-based skipping, its deliverable capacity \mathbb{C}_{rc}^{dp} is minimized when the cell strings are used to support the load sequentially, specifically,*

$$\mathbb{C}_{rc}^{dp} \geq (V \cdot I_C/P)^{\alpha-1} \sum_{i=1}^{k^{dp}} C_i = (V \cdot I_C/P)^{\alpha-1} \mathbb{C}_{ideal}^{dp}.$$

Finally, combining Theorem 5.3 and 5.4 leads to the following theorem on the near-optimality of the DP-based cell skipping in capacity delivery.

THEOREM 5.5. *The DP-based skipping achieves near-optimal capacity delivery of the battery pack, specifically,*

$$\frac{\mathbb{C}_{rc}^{dp}}{\mathbb{C}_{rc}^*} \geq \frac{(V \cdot I_C/P)^{\alpha-1} \mathbb{C}_{ideal}^{dp}}{(V \cdot I_C/P)^{\alpha-1} \lfloor \frac{n}{m} \rfloor^{\alpha-1} \mathbb{C}_{ideal}^{dp}} = \frac{1}{\lfloor \frac{n}{m} \rfloor^{\alpha-1}}.$$

Furthermore, we observe that (i) Theorem 5.5 is tight, as the equality establishes when the configuration identified by the DP-based method skips no cells and all the strings have the same capacity delivery; (ii) the configuration identified by the DP-based method approaches the optimal case with a smaller Peukert coefficient α . Figures 13 and 14 illustrate the near-optimality ratios according to Theorem 5.5 with regard to n , m , and α .

The fact that the DP-based cell skipping identifies the configuration with the maximum capacity delivery for ideal cells also implies a few cases in which the maximum capacity delivery can be guaranteed even when rate-capacity effect is considered.

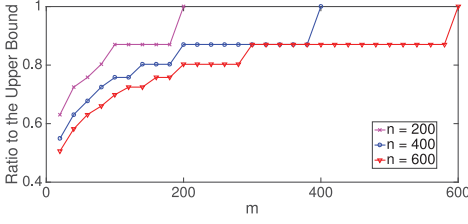


Fig. 13. Illustration of Theorem 5.5 with respect to n and m .

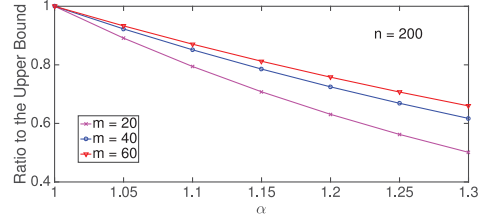


Fig. 14. Illustration of Theorem 5.5 with respect to α .

THEOREM 5.6. *Even when considering rate-capacity effect, the DP-based cell skipping achieves optimal capacity delivery of the battery pack when*

$$\frac{n - \sum S_{1 \times n}^{\text{dp}}}{m} = \left\lfloor \frac{n}{m} \right\rfloor, \quad (5)$$

or

$$\frac{n - \sum S_{1 \times n}^{\text{dp}}}{m} < \left\lfloor \frac{n}{m} \right\rfloor \text{ and } \left(\frac{n - \sum S_{1 \times n}^{\text{dp}}}{m} \right)^{\alpha-1} \mathbb{C}_{\text{rc}}^{\text{dp}} \geq \left\lfloor \frac{n}{m} \right\rfloor^{\alpha-1} \sum_{i=1}^n c_i. \quad (6)$$

Condition (5) captures the cases that $S_{1 \times n}^{\text{dp}}$ forms the maximum number of parallel strings, thus reducing the discharge current as much as possible. Condition (6) captures the cases that, although fewer parallel strings are formed with $S_{1 \times n}^{\text{dp}}$, its advantage in capacity delivery with ideal cells are strong enough to compensate the loss caused by rate-capacity effect (e.g., when the skipped cells are very weak). This way, the GA-based improvement only needs to be run when neither Condition (5) nor Condition (6) holds, reducing CSR's average computation complexity, especially in view of the fact that the GA-based improvement contributes a larger part to its overall execution time, as will be seen in Section 6.

5.2. Step II: GA-Based Improvement

We have shown the DP-based cell skipping identifies the configuration (i.e., $S_{1 \times n}^{\text{dp}}$) with near-optimal capacity delivery and, indeed, achieves the optimal capacity delivery in certain cases. Next, we further improve $S_{1 \times n}^{\text{dp}}$ heuristically with GA (if needed). Mimicking the natural selection process, GA is widely used to generate promising solutions to optimization and search problems—a population of candidate solutions, referred to as individuals, is evolved toward better solutions, and the initial populations greatly affect how fast the evolving process converges [Banzhaf et al. 1998].

We use GA to improve $S_{1 \times n}^{\text{dp}}$ because (i) the fact that any system configuration can be represented by a bit vector $S_{1 \times n}$ —similar to the individual representation in GA—facilitates to formulate the problem under the GA framework; (ii) with the near-optimal $S_{1 \times n}^{\text{dp}}$, we can generate competitive initial populations to make the evolving process converge quickly. Figure 15 summarizes the logic flow of the GA implementation.

—*Population Pool.* A population pool with N individuals is adopted, including $S_{1 \times n}^{\text{dp}}$ and the configuration when no cells are skipped— $S_{1 \times n}^{\text{all}} = \{0\}_{1 \times n}$. The remaining $(N - 2)$ individuals are randomly generated conforming to

$$\text{mod} \left(\sum_{i=1}^n S_{1 \times n}(i), m \right) = 0.$$

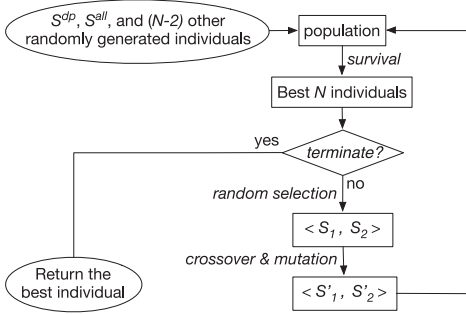


Fig. 15. Logic flow of the GA improvement.

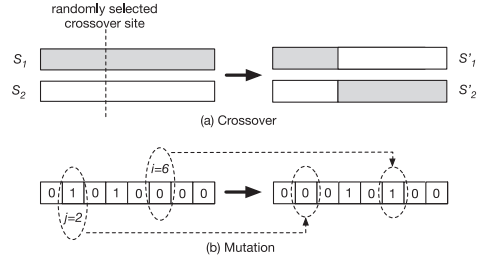


Fig. 16. Crossover and mutation.

- Fitness Function.* The fitness of individuals is defined as their respective deliverable capacity.
- Selection, Crossover, and Mutation.* M pairs of parents are selected randomly from the population pool for each generation, with which crossover is performed at a random crossover site (Figure 16(a)). Note, if $\text{mod}(\sum_{i=1}^n S_{1 \times n}(i), m) = x \neq 0$ for an offspring, its weakest x cells with $S_{1 \times n}(i) = 1$ are further skipped. The offspring are mutated by flipping a randomly selected $\{i \mid S_{1 \times n}(i) = 0\}$ to $S_{1 \times n}(i) = 1$ and another randomly selected $\{j \mid S_{1 \times n}(j) = 1\}$ to $S_{1 \times n}(j) = 0$ (Figure 16(b)).
- Survival.* The offspring in each generation are added to the pool and the N individuals with the best fitness survive to the next generation. The evolving process terminates when reaching a pre-defined number of generations.

As both $S_{1 \times n}^{\text{dp}}$ and $S_{1 \times n}^{\text{all}}$ are included in the initial population, we know the capacity delivery of the configuration identified by the GA implementation $\mathbb{C}_{\text{rc}}^{\text{CSR}}$ satisfies

$$\mathbb{C}_{\text{rc}}^{\text{CSR}} \geq \max \{ \mathbb{C}_{\text{rc}}^{\text{dp}}, \mathbb{C}_{\text{rc}}^{\text{all}} \}.$$

5.3. Salient Properties of CSR

5.3.1. CSR Rebalances Cells in the Long Run. CSR is motivated by the cell imbalance issue in battery packs. Besides improving the battery pack's capacity delivery during individual discharge cycles, CSR also reduces the cell imbalance in the pack over extended operation cycles. This is because (i) cells' capacity decreases over cycling and (ii) CSR rests weaker cells and thus slows down their capacity fading, allowing cells to rebalance. We will elaborate more on this in Section 6.2.

5.3.2. CSR is not Confined to JPL-Type Battery Packs. The core operation of CSR is the DP-based cell skipping, which is based on the sequential properties of cells in JPL-type battery packs. Here, we would emphasize that the sequential properties of cells are not only confined to JPL-type battery packs, but are shared by, to the best of our knowledge, all reconfigurable battery packs with a single pair of power buses (e.g., Kim and Shin [2009], Ci et al. [2012a], and Jin and Shin [2012]). This is because these sequential properties are imposed by the physical laws—the physical direction of discharge current leads to the intra-string sequential property and the physical protection of cells from short leads to the inter-string sequential property. For example, Figure 17 shows our reconfigurable battery board prototype, with which four battery cells, conforming to the intra-string sequential property, can be selectively used to form a string. Another example where both the intra- and inter-sequential properties hold is Kim and Shin [2009].



Fig. 17. Reconfigurable battery board prototype.



Fig. 18. Experiments lab settings.

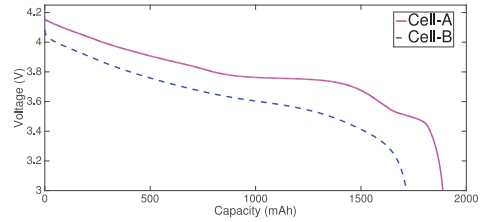


Fig. 19. Exemplary discharge traces.

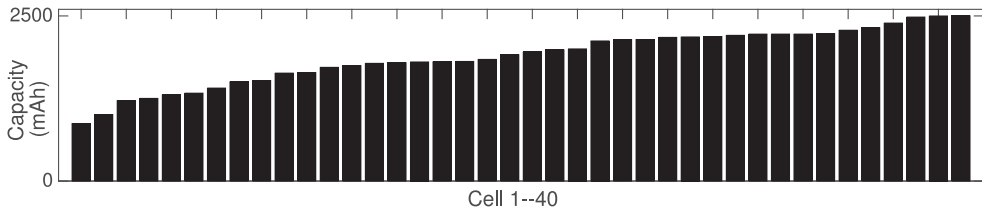


Fig. 20. Deliverable capacity of 40 lithium-ion cells when discharged with 1C rate.

5.3.3. CSR Goes Beyond Peukert's Law. Peukert's law is classic for representing the relationship between the discharge rate and cells' capacity delivery, especially for a constant discharge rate as in the system model shown in Figure 7. However, it is known that the accuracy of Peukert's law degrades when the discharge rate varies over time [Omar et al. 2013]. Fortunately, CSR still applies to such variable discharge rates' scenarios because (i) the DP-based cell skipping does not consider the rate-capacity effect and thus is not affected by variable discharge rates; (ii) instead of using Peukert's law, we can re-define the GA's fitness function based on more advanced analytical/circuit battery models (e.g., Kim [2012] and Bergveld et al. [2002]), and the other parts of the GA implementation remain identical. The accuracy of Peukert's law, however, does affect the performance analysis presented in Section 5.1.3.

6. EVALUATION

We have evaluated CSR by emulating battery packs with empirically collected cell discharge traces. We have also investigated the sensitivity of CSR over cell imbalance degree via Monte Carlo simulations.

6.1. Trace-Driven Emulation

We collect 40 rechargeable lithium-ion cells, and then fully charge and discharge them individually with 1C rate with the NEWARE battery tester as shown in Figure 18, which allows not only high accuracy charge/discharge control (with errors $<0.2\%$), but also fine-grained logging of the experiments (up to 10Hz). Figure 19 shows two exemplary thus-collected discharge traces. Figure 20 summarizes the capacity delivery of these cells ascendingly.

We emulate JPL-type battery packs with these traces—each cell in the pack is randomly emulated to be one of these 40 cells in Figure 20. Table I lists the default settings unless specified otherwise. For the GA-implementation, a population of 2,000 individuals is used and the evolving process terminates after 1,000 generations. The emulator is implemented with Matlab. The reported results are averaged over 500 runs.

Table I. Default Emulation Settings

Pack Scale	Peukert Coeff.	String Size	Load Current
1,000	1.2	15	5C

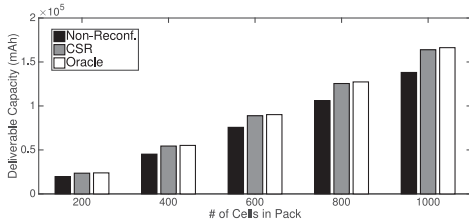


Fig. 21. Capacity delivery with various battery pack scales.

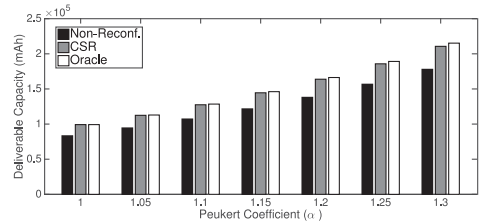


Fig. 22. Capacity delivery with various Peukert coefficients.

We also emulate non-reconfigurable battery packs in which no cells could be skipped—the first m cells in the pack form the first string, the second m cells form the second string, and so on. The Oracle capacity delivery calculated according to Theorem 5.3 is also explored for comparison.

6.1.1. Impact of Battery Pack Scale. Figure 21 plots the capacity delivery of battery packs consisting of 200–1,000 cells. The JPL-type battery pack with CSR delivers more capacity than the non-reconfigurable packs for all explored cases, especially for large battery packs. For example, CSR delivers 25,788mAh more capacity than the non-reconfigurable case for 1,000-cell battery packs. This indicates CSR is particularly desirable for large battery systems such as EVs. Also, CSR achieves close capacity delivery to the Oracle solution—although the gap between CSR and Oracle increases with larger battery pack scales, a performance ratio of 98.6% is achieved even for the 1,000-cell battery packs.

6.1.2. Impact of Peukert Coefficient. Figure 22 shows the capacity delivery with various Peukert coefficients, from which two observations can be made. First, compared to the non-reconfigurable case, the advantage of CSR pronounces for cells with small Peukert coefficients. For example, the capacity delivery is improved by 20% with an α of 1.00, which reduces to $\approx 17\%$ with $\alpha = 1.30$. Second, CSR achieves the Oracle capacity delivery when cells are ideal (i.e., when $\alpha = 1$), and its gap to the Oracle solution increases as α increases. However, even with $\alpha = 1.30$, CSR still achieves a performance ratio of 97.9% when compared to Oracle. Both these observations indicate that CSR works better for cells with a smaller Peukert coefficient, which is also the direction of battery development as cells with smaller α indicate good efficiency and less loss.

6.1.3. Impact of Load Required Discharge Rate. Figure 23 plots the capacity delivery with various load required current. CSR outperforms the non-reconfigurable battery packs, especially with smaller load required discharge rates. For example, about 22,577mAh more capacity is delivered with a 10C load current, which increases to 31,053mAh when the load current reduces to 2C. This is because larger load currents pronounce the rate-capacity effect, which is ignored by the DP-based cell skipping. This way, the advantage of CSR diminishes as the load current increases. However, CSR improves the capacity delivery by $\approx 19\%$ even with 10C load current. CSR achieves a performance ratio of $\approx 98\%$ when compared to the Oracle, agreeing with Figure 21.

Table II. Number of Parallel Strings

String Size (m)	5	10	15	20	25
CSR	192.35	93.83	61.62	45.71	36.27
Maximum ($\lfloor \frac{n}{m} \rfloor$)	200	100	66.67	50	40
Skipped Cells	38.25	61.70	75.70	85.80	93.25

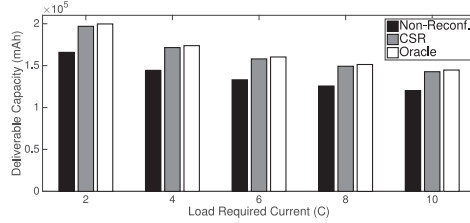


Fig. 23. Capacity delivery with various load required discharge rates.

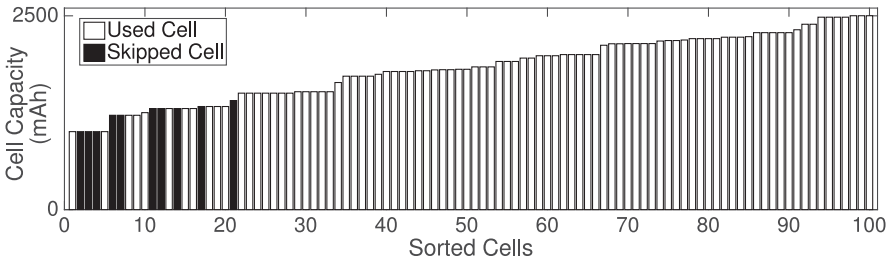


Fig. 24. CSR skips weak cells but not necessarily the weakest ones.

6.1.4. Number of Formed Strings. Clearly, skipping cells from discharge leads to fewer cell strings when compared to using all the cells to support the load. Table II lists the average number of parallel strings formed by CSR with various load required string sizes. We also list the maximum number of parallel strings for comparison (i.e., $\lfloor \frac{n}{m} \rfloor$). Not surprisingly, fewer strings are formed with CSR. Multiplying the reduction in the number of formed strings and the corresponding required string size, we can see more cells are skipped when the load requires longer strings. For example, $(40 - 36.27) \times 25 = 93.25$ cells are skipped on average when 25-cell strings are required, while only $(200 - 192.35) \times 5 = 38.25$ cells are skipped for the 5-cell string case. Again, this indicates the selective cell skipping is especially important for high voltage load applications (i.e., requiring longer cell strings) such as EVs.

6.1.5. Skipped Cells Distribution. CSR is inspired by the observation that selectively skipping weak cells from discharge may improve the battery pack's capacity delivery; however, CSR does not simply skip the weakest cells. To demonstrate the difference between CSR and the greedy cell skipping, Figure 24 plots the skipped cells in an emulated 100-cell battery pack.⁵ By ascendingly sorting the cells according to their respective deliverable capacity, we find, although the skipped cells by CSR are clustered at the low capacity spectrum, they are not simply the weakest ones. Specifically, for this particular battery pack, CSR identifies a configuration with 9,849mAh deliverable capacity, while that with the greedy approach delivers only 9,509mAh.

⁵The relatively small battery pack scale is to ease the observation in Figure 24.

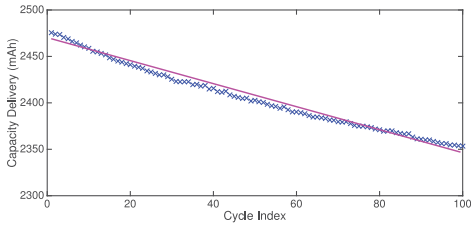


Fig. 25. Cells' fading over cycling.

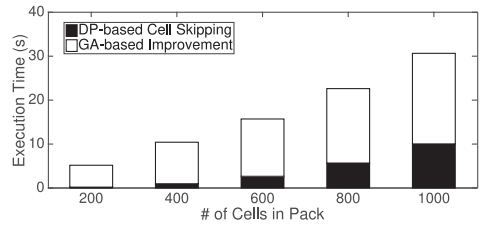


Fig. 26. Execution time of CSR.

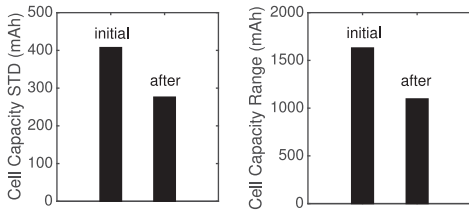


Fig. 27. CSR rebalances cells over usage.

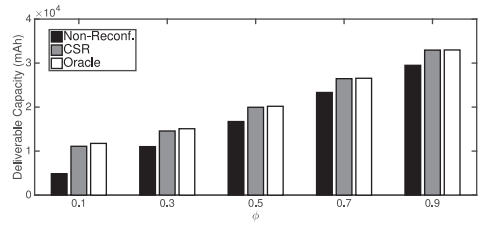


Fig. 28. Sensitivity of CSR over cell imbalance.

6.1.6. Execution Time. Figure 26 plots the execution time of CSR with a 2.5GHz Intel Core i5 processor. The execution time is contributed more by the GA implementation, especially when the battery pack size is relatively small. This shows another advantage of CSR, as the GA method is used only when the configuration identified by DP is not optimal (as illustrated in Figure 11).

6.2. CSR Rebalances Cells

Next, we verify the fact that CSR rebalances cells in the long run, as explained in Section 5.3. Figure 25 plots our 15-day measurements on the capacity fading of a lithium-ion cell over 100 charge/discharge cycles, showing (i) a cell's capacity fades linearly, agreeing with the reported findings in the literature [Lam and Bauer 2013], and (ii) a total fading of 5% over these 100 cycles, or 0.05% fading per cycle. With this per-cycle fading rate, and assuming a load required string size of 20 and current of 5C, we emulate a 500-cycle charging/discharging test of a 600-cell JPL-type battery pack, during which CSR is used to determine the desired configuration. Figure 27 compares the cell imbalance when the emulation begins with that after the cycling test, in terms of both the standard deviation of cell capacities and their ranges (i.e., the difference between the maximum and minimum capacity of cells), showing that by allowing the weak cells to rest, CSR reduces the differences among cell capacities by over 30%.

6.3. Sensitivity Analysis over Cell Imbalance

CSR is inspired by the wide existence of cell imbalance in battery packs. Next, we investigate the sensitivity of CSR over cell imbalance degree. To capture the cell imbalance degree, we introduce a control parameter ϕ ($\phi \in [0, 1]$) and randomly generate the cell capacity under 1C rate in the range of $[\phi, 1] \times c_0$, where c_0 is the rated capacity of cells and specifically, 2,300mAh in our settings. This way, a smaller ϕ indicates higher cell imbalance in the battery pack. We apply CSR to JPL-type battery packs, and again, compare it to the non-reconfigurable battery packs and the Oracle solution. Figure 28 plots the collected results averaged over 500 runs. Not surprisingly, the advantage of CSR over the non-reconfigurable case is pronounced with larger cell

imbalance degree (e.g., about $> 100\%$ improvement with a ϕ of 0.1). Note, this small ϕ can be interpreted as the case that certain cells fail over usage, which is commonly found in practice [Berman 2012; AA1Car 2016]. CSR approaches the Oracle as cells become more balanced.

7. FURTHER DISCUSSION

7.1. Skip or Not?—A Necessary Condition

Next, we present a necessary condition that helps to determine whether cell skipping should be performed to enhance the capacity delivery of the battery pack.

Denote c_{\min} and c_{\max} as the capacity delivery of the weakest and strongest cells in the pack, respectively. Clearly, a lower bound of the deliverable capacity when all cells are used C_{\min}^{all} is

$$C_{\min}^{\text{all}} \geq c_{\min} \cdot \left\lfloor \frac{n}{m} \right\rfloor. \quad (7)$$

Similarly, an upper bound of the deliverable capacity when x cells are skipped from discharge $C_{\max}^{\text{skip}}(x)$ is

$$C_{\max}^{\text{skip}}(x) \leq c_{\max} \cdot \left\lfloor \frac{n-x}{m} \right\rfloor \leq c_{\max} \cdot \left\lfloor \frac{n-1}{m} \right\rfloor. \quad (8)$$

Combining Conditions (7) and (8), we know

$$\frac{C_{\max}^{\text{skip}}}{C_{\min}^{\text{all}}} \leq \frac{C_0 \cdot c_{\max} \cdot \left\lfloor \frac{n-1}{m} \right\rfloor}{C_0 \cdot c_{\min} \cdot \left\lfloor \frac{n}{m} \right\rfloor} = \frac{c_{\max} \cdot \left\lfloor \frac{n-1}{m} \right\rfloor}{c_{\min} \cdot \left\lfloor \frac{n}{m} \right\rfloor}.$$

As a result, a necessary condition for skipping cells to improve the capacity delivery (i.e., $\frac{C_{\max}^{\text{skip}}}{C_{\min}^{\text{all}}} > 1$) is

$$\left\lfloor \frac{n-1}{m} \right\rfloor \Big/ \left\lfloor \frac{n}{m} \right\rfloor > \frac{c_{\min}}{c_{\max}}. \quad (9)$$

7.2. Module-Level Reconfigurability: Tesla S as an Example

This article is presented assuming the cell-level reconfigurability—the connectivity of individual cells can be actively adjusted according to the design of JPL. The reconfigurability, however, is achieved by equipping cells with switches, increasing system cost and complexity. A tradeoff between system reconfigurability and cost can be achieved by exploring the module-level reconfiguration [Alahmad et al. 2008].

Let us consider the 85kWh battery pack of Tesla S. The battery pack consists of 7,104 lithium-ion cells, with which 74 parallel cell strings are formed, each with 96 cells connected in series to supply an operating voltage of around 403V. Again, we randomly emulate the capacity delivery of these 7,104 cells based on Figure 20, and Figure 29 shows the power capability of this non-reconfigurable battery pack. Next, we emulate the module-level reconfigurable JPL-type battery pack with the same 7,104 cells with module size l ($l \in [1, 96]$)—each module consists of l cells connected in series. This way, $l = 1$ is the case of cell-level reconfiguration as discussed in the article and $l = 96$ corresponds to the case of non-reconfigurable battery packs. The power capability of thus-emulated JPL-type battery packs with varying l is also shown in Figure 29. As expected, the advantage of CSR pronounces with smaller module size, and the extreme case of $l = 1$ shows a 43% improvement in power capability. This, however, is at the cost of more switches and higher wiring complexity of the battery pack. Larger module size reduces the complexity in exchange for the pack's reconfigurability and thus power capability.

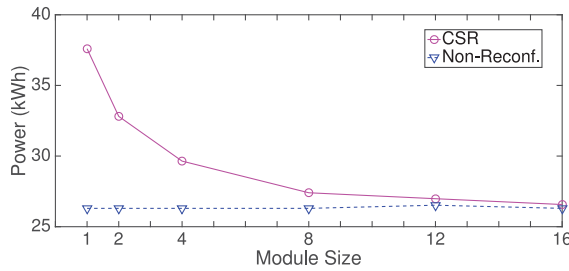


Fig. 29. Trading off system complexity and capacity delivery via exploring module-level reconfiguration.

8. RELATED WORK

In general, existing studies of reconfigurable battery packs can be classified into two categories: *offering* reconfigurability and *exploiting* reconfigurability.

8.1. Design of Reconfigurable Battery Packs

The system reconfigurability is achieved by adding switches into the battery pack and thus increases system complexity. Much research effort has been devoted to achieve high reconfigurability with low system complexity [Ci et al. 2012b]. Kim et al. [2012] proposed a reconfigurable battery pack design in which each cell is equipped with two switches—one for connecting the cell to the load and the other for skipping the cell. With this design, any subset of cells can be sequentially connected in series, but no parallel strings can be formed. A reconfigurable battery pack where three switches are equipped for individual cells is designed in Kim and Shin [2010]. The JPL-type battery pack [Alahmad et al. 2008] considered in this article allows for forming multiple parallel strings by equipping four switches to each cell. Increasing the per-cell switches to six, a reconfigurable battery pack supporting multiple outputs was proposed in Kim and Shin [2009].

8.2. Reconfiguration-Assisted Optimization

The other category of existing work on reconfigurable battery packs focuses on exploitation of the offered reconfigurability to improve the battery performance. For example, a reconfiguration algorithm by matching the supplied and required voltages, and thus reducing the energy loss due to voltage regulation, was presented in He et al. [2013]. The tradeoff between cycle efficiency and capacity utilization of the battery pack was explored in Kim et al. [2011]. A set of discharge management policies for reconfigurable battery packs is proposed and validated in Raychev et al. [2011]. Molenaar exploited the battery reconfiguration to achieve the fast charging of vehicles in Modenaar [2010]. The reconfiguration-assisted charging of battery packs was explored in He et al. [2014]. The integration of different kinds of batteries via reconfiguration is explored in Badam et al. [2015].

8.3. CSR's Position

CSR belongs to the second category on exploiting reconfiguration for system optimization, and differs from existing works by mitigating cell imbalance based on a particular design of the JPL-type battery packs. Cell imbalance is traditionally mitigated by top-balancing (i.e., balancing cells in fully charged state), bottom-balancing (i.e., balancing cells in the discharged state), dissipative balancing (i.e., dissipating energy from strong cells during discharging), and non-dissipative balancing (i.e., redistributing energy between strong and weak cells to make them balance) [Barsukov and Qian 2013]. These approaches form two clusters based on the resultant capacity delivery:

the pack capacity is dominated by the weakest cells in the first three approaches, and the non-dissipative balancing makes full use of cells' capacity in the ideal case. CSR is orthogonal to the first clusters, for example, the cell capacity in Figure 10 can be treated as the resultant capacity delivery after top-balancing. Also, different from non-dissipative balancing that redistributes energy among cells, CSR balances cells from another perspective by redistributing their loads via reconfiguration. To the best of our knowledge, the most similar works to CSR are Ci et al. [2012a] and He et al. [2015]. Ci et al. [2012a] uses reconfiguration to enhance the energy utilization of the battery pack via a Lagrangian relaxation, but without directly considering the rate-capacity effect. We have presented a general approach to mitigate cell imbalance via reconfiguration based on a graph model and show its NP-hardness in He et al. [2015]. CSR advances the state of the art with the JPL-type battery packs, whose cells show two sequential properties that significantly simplify the reconfiguration algorithm (i.e., facilitating a DP-based solution).

9. CONCLUSION

In this article, we presented a case study of mitigating cell imbalance in battery packs via system reconfiguration. We abstracted the problem of identifying the configuration with maximum capacity delivery to a cell-selection problem based on two sequential properties of cells in the battery pack. Then, we presented CSR, a two-step reconfiguration algorithm that identifies a near-optimal configuration with DP first and then GA. Our trace-driven emulation shows CSR achieves the optimal capacity delivery when the cell imbalance is low and improves the battery pack's capacity delivery by up to 1x in case of high imbalance.

REFERENCES

- AA1Car. 2016. Honda Civic Hybrid Battery Failure. (Retrieved from http://www.aa1car.com/library/honda_civic_hybrid_battery.htm).
- Mahmoud Alahmad, Herb Hess, Mohammad Mojarradi, William West, and Jay Whitacre. 2008. Battery switch array system with application for JPL's rechargeable micro-scale batteries. *Journal of Power Sources* 177, 2 (2008), 566–578.
- Anirudh Badam, Ranveer Chandra, Jon Dutra, Anthony Ferrese, Steve Hodges, Pan Hu, Julia Meinershagen, Thomas Moscibroda, Bodhi Priyantha, and Evangelia Skiani. 2015. Software defined batteries. In *SOSP'15*.
- Wolfgang Banzhaf, Peter Nordin, Robert Keller, and Frank Francone. 1998. *Genetic Programming – An Introduction*. Morgan Kaufmann.
- Yevgen Barsukov and Jinrong Qian. 2013. *Battery Power Management for Portable Devices*. Artech House, Chapter 4.
- D. Belov and Mo-Hua Yang. 2008. Failure mechanism of Li-ion battery at overcharge conditions. *Journal of Solid State Electrochemistry* 12, 7 (2008), 885–894.
- Henk Jan Bergveld, Wanda S. Kruijt, and Peter H. L. Notten. 2002. *Battery Management Systems: Design by Modeling*. Kluwer Academic.
- Bradley Berman. 2012. Tesla Battery Failures Make Bricking a Buzzword. Retrieved from <http://www.nytimes.com/2012/03/04/automobiles/Tesla-Battery-Failures-Make-Bricking-a-Buzzword.html>.
- S. Chandra, D. F. Gayme, and A. Chakraborty. 2014. Coordinating wind farms and battery management systems for inter-area oscillation damping: A frequency-domain approach. *IEEE Transactions on Power Systems* 29, 3 (May 2014), 1454–1462. DOI : <http://dx.doi.org/10.1109/TPWRS.2013.2282367>
- Song Ci, Jiucui Zhang, Hamid Sharif, and Mahmoud Alahmad. 2012a. Dynamic reconfigurable multi-cell battery: A novel approach to improve battery performance. In *APEC'12*.
- Song Ci, Jiucui Zhang, Hamid Sharif, and Mahmoud Alahmad. 2012b. A novel design of adaptive reconfigurable multiple battery for power-aware embedded networked sensing systems. In *GLOBECOM'12*.
- Lee H. Goldberg. 2011. Battery cell balancing for improved performance in EVs. *Electronic Products Magazine* (2011).

- Liang He, Lipeng Gu, Linghe Kong, Yu Gu, Cong Liu, and Tian He. 2013. Exploring adaptive reconfiguration to optimize energy efficiency in large-scale battery systems. In *RTSS'13*.
- Liang He, Yu Gu, Cong Liu, Ting Zhu, and Kang G. Shin. 2015. SHARE: SoH-aware reconfiguration to enhance deliverable capacity of large-scale battery packs. In *ICCPs'15*.
- Liang He, Eugene Kim, and Kang G. Shin. 2016. Resting weak cells to improve battery pack's capacity delivery via reconfiguration. In *ICCPs'16*.
- Liang He, Linghe Kong, Siyu Lin, Shaodong Ying, Yu Gu, Tian He, and Cong Liu. 2014. Reconfiguration-assisted charging in large-scale Lithium-ion battery systems. In *ICCPs'14*.
- Fangjian Jin and Kang G. Shin. 2012. Pack sizing and reconfiguration for management of large-scale batteries. In *ICCPs'12*.
- Hahnsang Kim and Kang G. Shin. 2009. On dynamic reconfiguration of a large-scale battery system. In *RTAS'09*.
- Hahnsang Kim and Kang G. Shin. 2010. Dependable, efficient, scalable architecture for management of large-scale batteries. In *ICCPs'10*.
- Taesic Kim. 2012. A hybrid battery model capable of capturing dynamic circuit characteristics and nonlinear capacity effects. Master Thesis, University of Nebraska-Lincoln.
- Taesic Kim, Wei Qiao, and Liyan Qu. 2012. A series-connected self-reconfigurable multicell battery capable of safe and effective charging/discharging and balancing operations. In *APEC'12*.
- Younghyun Kim, Sangyoung Park, Yanzhi Wang, Qing Xie, Naehyuck Chang, Massimo Poncino, and Massoud Pedram. 2011. Balanced reconfiguration of storage banks in a hybrid electrical energy storage system. In *ICCAD'11*.
- Long Lam and Pavol Bauer. 2013. Practical capacity fading model for Li-Ion battery cells in electric vehicles. *IEEE Transactions on Power Electronics* 28, 12 (2013), 5910–5918.
- B. A. M. Modenaar. 2010. Reconfigurable battery system for ultra fast charging of industrial electric vehicles. *Master Thesis, Delft University of Technology* (2010).
- Noshin Omar, Peter Van den Bossche, Thierry Coosemans, and Joeri Van Mierlo. 2013. Peukert revisited: Critical appraisal and need for modification for Lithium-Ion batteries. *Energies* 6, 11 (2013), 5625–5641. DOI: <http://dx.doi.org/10.3390/en6115625>
- Delyan Raychev, Youhuizi Li, and Weisong Shi. 2011. The seventh cell of a six-cell battery. In *WEED'11*.
- K. Vatanparvar and M. A. Al Faruque. 2015. Battery lifetime-aware automotive climate control for electric vehicles. In *DAC'15*.
- H. Visairo and P. Kumar. 2008. A reconfigurable battery pack for improving power conversion efficiency in portable devices. In *ICCDs'08*.
- WPSAC. 2007. Understanding “Arc Flash.” Retrieved from https://www.osha.gov/dte/grant_materials/fy07/sh-16615-07/arc_flash_handout.pdf.

Received June 2016; revised November 2016; accepted December 2016